

Brilliant Glyconanocapsules for Trapping of Bacteria

Xibo Yan,¹ Adeline Sivignon,^{2,3} Pierre Alcouffe,¹ Béatrice Burdin,⁴ Sabine Favre-Bonté,⁵ Rostyslav Bilyy,⁶ Nicolas Barnich,^{2,3} Etienne Fleury,¹ François Ganachaud¹ and Julien Bernard^{1,*}

¹ Université de Lyon, Lyon, F-69003, France ; INSA-Lyon, IMP, Villeurbanne, F-69621, France; CNRS, UMR 5223, Ingénierie des Matériaux Polymères, Villeurbanne, F-69621, France.

² Clermont Université, UMR 1071, Inserm/Université d'Auvergne, 63000 Clermont-Ferrand, France.

³ INRA, Unité Sous Contrat 2018, 63000, Clermont-Ferrand, France.

⁴ Centre Technologique des Microstructures (CTμ), Université Claude Bernard Lyon 1, France.

⁵ Université de Lyon, France Research Group on "Bacterial Opportunistic Pathogens and Environment". UMR 5557 Ecologie Microbienne, CNRS, Vetagro Sup and Université Lyon1, France.

⁶ Friedrich-Alexander University of Erlangen-Nürnberg, Department of Internal Medicine 3-Rheumatology and Immunology, D-91054 Erlangen, Germany.

Table of contents

Materials	2
Methods	2
Synthesis of N-[5-(β-D-glucopyranosyloxy)3-oxapentyl]methacrylamide	4
Preparation of glyco-copolymers	10
Phase diagrams' determination	12
Preparation of glyconanocapsules by co-nanoprecipitation/polymer crosslinking	13
Encapsulation of hydrophobic active components	15
Post-nanoprecipitation modification	16
Cytotoxicity tests	17
Mannosylated Glyconanocapsules induced Bacteria Aggregation	19
Removal of bacteria	19
Residual adhesion	20
Control experiment	20
References	21

Materials

4-Cyano-4-(phenylcarbonothioylthio) pentanoic acid (CPADB, 97%, HPLC), 4,4'-Azobis (4-cyanovaleric acid) (ACPA, 98%), isophorone diisocyanate (IPDI, 98%), hexadecane (99%), water (HPLC), deuterium oxide (D₂O), avidin from egg white (min 98%), pyrene (98%), Dulbecco's PBS buffer were purchased from Sigma Aldrich, and used without further purification. 2,2-Azobis(4-methoxy-2,4-dimethyl-valeronitrile) (V70, min 95%) was purchased from Wako pure chemical industries. Cystamine was obtained from protonated cystamine dihydrochloride (Sigma Aldrich, 98%) by adding 3 eq. of triethylamine (Sigma Aldrich, 99%). Amino-functionalized biotin was obtained from protonated biotin ethylenediamine hydrobromide (Sigma Aldrich, 95%) by adding 1.5 eq. of triethylamine (Sigma Aldrich, 99%). Miglyol 812 was purchased from SASOL (Germany). Acetone (99.5%) and methanol (99.8%) were purchased from Carlo Erba. Dialysis membranes (Mw cut-off 1000 Da) were purchased from Spectrum Laboratories, Inc. Alexa Fluor® 555 Cadaverine was purchased from Life technologies and Turbo beads PEG amine was purchased from TurboBeads. Other reactants were purchased from Sigma-Aldrich. N-[7-(α -D-mannopyranosyloxy)heptyl] methacrylamide (HMM) was prepared as described in the literature.¹ The AIEC reference strain LF82 was isolated from CD patients. To visualize AIEC LF82 bacteria by fluorescence, bacteria were transformed with the plasmid pFPV25.1, which harbours the green fluorescent protein (GFP). Bacteria were grown routinely in Luria–Bertani (LB) broth or on LB agar plates overnight at 37°C.

Methods

Nuclear magnetic resonance (NMR) spectra were recorded on a Bruker Avance III spectrometer (400 MHz) in DMSO solution at 300K and referenced to residual solvent peaks.

Acetylated glycopolymers were analyzed with a SEC apparatus running in THF at 25 (flow rate:1 mL/min) and equipped with a Viscotek VE1121 automatic injector, three columns (Waters HR2, HR1 and HR0.5), and a differential refractive index detector (Viscotek VE3580). The average molar masses of the glycopolymers were derived from a calibration curve based on a series of PS standards.

Particle size measurements were carried out by dynamic light scattering (DLS) using a Malvern Instruments Zetasizer nano series instrument and using the cumulant method. The aqueous solutions were prepared at 1 mg/mL, at least five measurements were made for each sample. Equilibration times of 10 minutes were respected before each measurement.

TEM images were obtained on a Philips CM120 electronic microscope, by observations in transmission at an accelerating voltage of 80 kV. Samples were made by placing a drop of sample (1 mg/mL) onto Formvar-coated copper grid. Excess solution was carefully blotted off using filter paper and samples were dried for a few minutes before analysis.

Fluorescence spectroscopy analyses were performed using a JASCO FP-8000 series spectrofluorometer. All the fluorescent spectra were measured in aqueous solution after dialysis of the glyconano-capsules at room temperature.

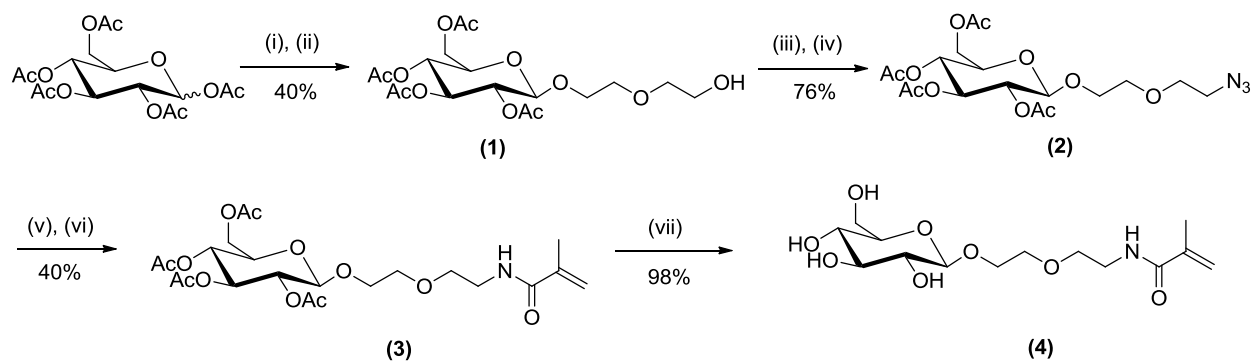
Fluorescence microscopy was performed using a confocal laser scanning microscope (ZeissLSM510META) with 488 nm (3.9% laser transmission) and 543 nm (47% laser transmission) excitation wavelength. Emission signals were collected between 505 and 530 nm for the GFP and 560 and 615 nm for the AlexaFluor 555 with a beam splitter at 545 nm. Micrographs were performed

with an apochromatic x63/1.4NA objective lens on slices of 1 μm (pinhole 1.4 Airy Unit) with a speed of 1.60 $\mu\text{sec/pixel}$. Control of free bacteria, and free glyconanocapsules were performed to prevent cross-talk.

The *E. coli* strain was grown in LB medium containing kanamycin (50 $\mu\text{g/ml}$) overnight without agitation at 37°C. The optical density of the ON culture was adjusted in LB medium in order to reach $\text{OD}_{620\text{nm}} = 0.6$.

Adhesion assays were performed with AIEC LF82 strain and intestinal epithelial cells T84. The intestinal epithelial cells T84 were seeded in 48-well tissue culture plates at a density of 1.5×10^5 cells/well and were incubated at 37 °C for 48h. AIEC LF82 bacteria were incubated for 1 h with the mannosylated glyconanocapsules at 0.006, 0.06, 0.6, 6 and 30 $\mu\text{g.mL}^{-1}$ respectively) then cells were infected with the mixture at a multiplicity of infection (MOI) of 10 bacteria per cell for 3 h. Monolayers were washed 3 times with phosphate buffer (PBS) and lysed with 1% Triton X-100 (Sigma) in deionized water. Samples were diluted and plated onto LB agar plates to determine the number of colony-forming units (CFU).

Synthesis of N-[5-(β-D-glucopyranosyloxy)3-oxapentyl]methacrylamide



(i) 33% HBr/AcOH 0°C; (ii) Diethylene glycol, Ag₂CO₃, DCM/CH₃CN (10/1), r.t.; (iii) PPh₃, NBS, DMF, 55°C; (iv) NaN₃, 85°C; (v) H₂, Pd/C, ethanol, p-TsOH, r.t.; (vi) Methacryloyl chloride, Triethylamine, DCM, r.t.; (vii) MeONa, MeOH, r.t.

Scheme S1: Route to glucose-functionalized methacrylamide

Synthesis of azido-functional glucoside (2)

Peracetylated-D-Glucose (10 g, 25.6 mmol) was added at 0°C into 10 mL of hydrobromic acid solution (33 wt% in acetic acid). The solution was stirred for 2h and subsequently poured into a saturated NaHCO₃ aqueous solution (10% Na₂SO₃). The solution was diluted with dichloromethane to reach a total volume of 500 mL. The organic layer was washed with water (3×500 mL), brine (500 mL) and dried. A yellow product was obtained after evaporation of dichloromethane. The crude compound was then dissolved in 100 mL of dichloromethane and diethylene glycol (54 g, 512 mmol) and Ag₂CO₃ (2 g, 7.3 mmol) were then added at 0°C into the solution. After 2 h, the solution was warmed up to room temperature and the solution was stirred overnight. The solution was filtered over celite and washed with water (3×500 mL). After removal of the solvent, the crude product (yellow gum) was purified by column chromatography (petroleum ether/ethyl acetate, 4/1, v/v) to afford compound **1**. Final yield: 4.5 g (40%) obtained as a colorless gum.

¹H NMR (400 MHz, CDCl₃) δ 5.21 (t, *J* = 9.2 Hz, 1H, H-3), 5.09 (t, *J* = 9.8 Hz, 1H, H-4), 5.02-4.97 (dd, *J* = 7.6, 9.2 Hz, 1H, H-2), 4.60 (d, *J* = 7.9 Hz, H-1), 4.27-4.23 (dd, *J* = 4.7, 12.3 Hz, 1H, H-6), 4.17-4.13 (dd, *J* = 2.4, 12.3 Hz, 1H, H-6'), 3.97-3.93 (m, 1H, OCH₂CH₂O), 3.76-3.64 (m, 6H, OCH₂CH₂O, H5, OCH₂CH₂OH), 3.59-3.56 (m, 2H, OCH₂CH₂OH), 2.08, 2.05, 2.02, 1.99 (s, 4×3H, 4×CH₃CO); ¹³C NMR (CDCl₃) δ 170.8, 170.4, 169.6, 169.5, 100.9, 72.9, 72.6, 72.0, 71.5, 70.2, 69.1, 68.6, 62.1, 61.8, 20.9, 20.8, 20.7, 20.7; ESI-MS: *m/z* calculated for [C₁₈H₂₈NO₁₂Na]⁺, 459.1473, found 459.1468.

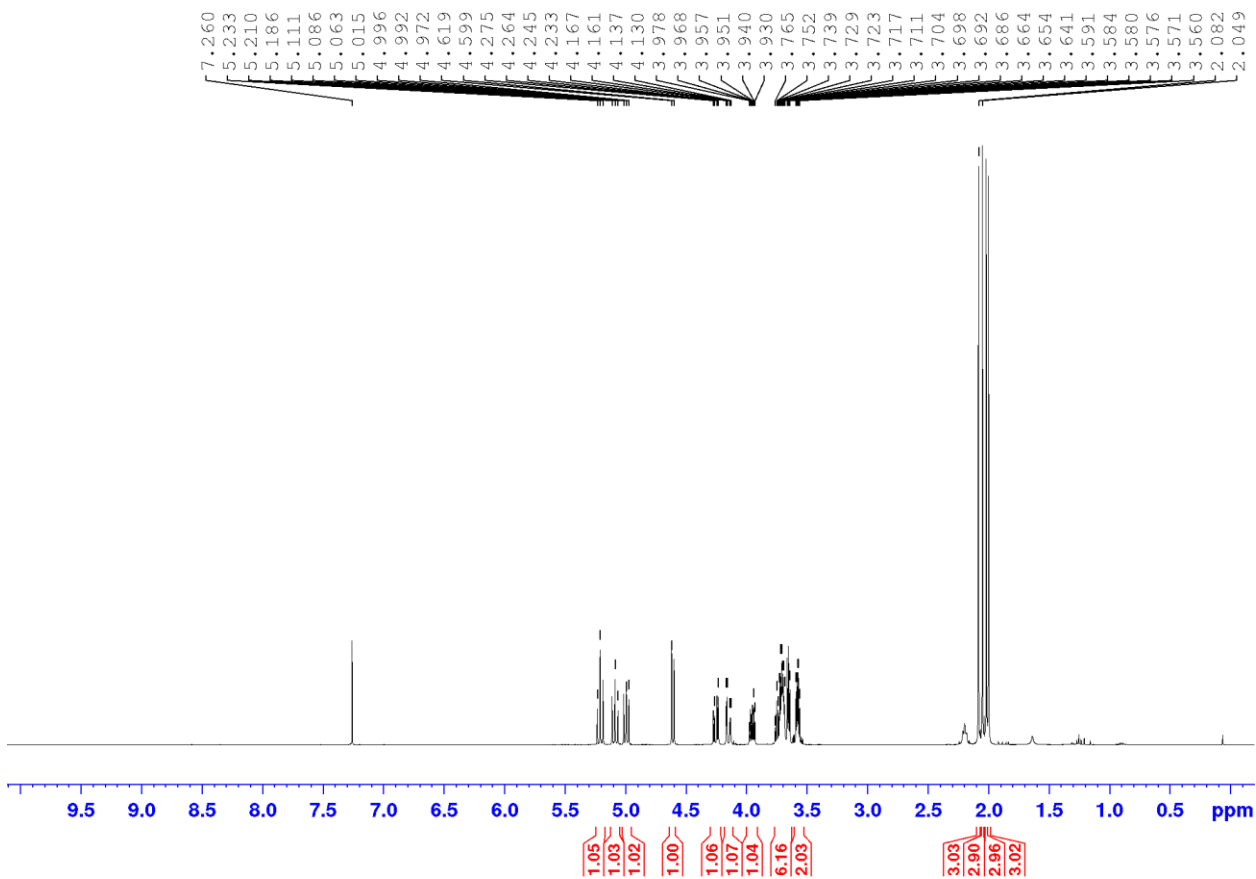


Figure S1: ^1H NMR of compound 1

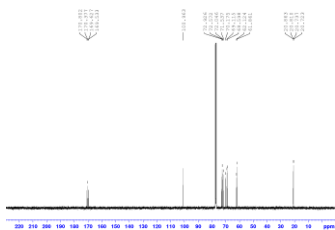


Figure S2: ^{13}C NMR of compound 1

1 (4 g, 9.2 mmol) and triphenylphosphine (6.8 g, 25.9 mmol) were dissolved in anhydrous DMF (100 mL) and the solution was cooled to 0°C. NBS (3.2 g, 17.9 mmol) was then added in the solution. After 20 min, the temperature was increased to 55°C and the solution was stirred for 4h. 20 mL of methanol were added to the solution and the solution was stirred for 10 min. Sodium azide (3.5 g, 53.8 mmol) was added into DMF solution. The mixture was stirred at 85 °C under argon for 24 h and cooled to room temperature. The solution was then diluted with EtOAc to reach a total volume of 1 L. The organic layer was washed with aq. NaHCO₃ (3×300 mL), water (3×300 mL), brine (300 mL) and dried. After concentration, the resulting product (yellow gum) was purified by column chromatography (petroleum ether/ethyl acetate, 2/1, v/v) to afford the corresponding azido-functionalized glucoside (**2**). Final yield: 3 g (76%) obtained as a colorless gum.

¹H NMR (400 MHz, CDCl₃) δ 5.21 (t, *J* = 9.4 Hz, 1H, H-3), 5.09 (t, *J* = 9.8 Hz, 1H, H-4), 5.02-4.97 (dd, *J* = 8.0, 9.6 Hz, 1H, H-2), 4.60 (d, *J* = 7.9 Hz, H-1), 4.27-4.23 (dd, *J* = 4.7, 12.3 Hz, 1H, H-6), 4.17-4.13 (dd, *J* = 2.4, 12.3 Hz, 1H, H-6'), 3.97-3.93 (m, 1H, OCH₂CH₂O), 3.78-3.64 (m, 6H, OCH₂CH₂O, H5, OCH₂CH₂N₃), 3.37-3.34 (m, 2H, OCH₂CH₂N₃), 2.08, 2.05, 2.02, 1.99 (s, 4×3H, 4×CH₃CO); ¹³C NMR (CDCl₃) δ 170.8, 170.4, 169.5, 169.5, 101.0, 73.0, 72.0, 71.5, 70.6, 70.4, 69.2, 68.6, 62.1, 50.9, 20.9, 20.8, 20.7, 20.7; ESI-MS: *m/z* calculated for [C₁₈H₂₇N₃O₁₁Na]⁺, 484.1538, found 484.1539.

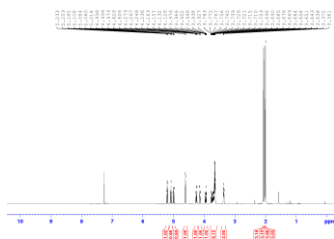


Figure S3: ¹H NMR of compound **2**

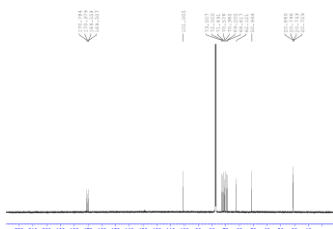


Figure S4: ^{13}C NMR of compound **2**

Synthesis of **4**

2 (3 g, 6.5 mmol), p-toluenesulfonic acid (1.4 g, 8.1 mmol) and 10% palladium on activated charcoal (1 g) as the catalyst were stirred overnight in ethanol (200 mL) at room temperature under 1 atm of hydrogen. The solution was filtered over celite and evaporated to obtain a colorless gum. The resulting product was directly engaged in the next step without further purification. The crude compound was dissolved in a solution of anhydrous CH_2Cl_2 (50 mL) containing triethylamine (3 mL). Methacryloyl chloride (1.08 mL) was added dropwise into a solution at 0°C . The solution was stirred for 1 h at room temperature. After reaction, the solution was washed with water (2x200 mL), dried over MgSO_4 and the solvent was removed. The acetylated monomer **3** was finally purified by column chromatography (petroleum ether/ethyl acetate, 2/3, v/v). Yield: 1.3 g (40%) of a colorless gum.

^1H NMR (400 MHz, CDCl_3) δ 6.31 (s, 1H, NH), 5.72 (s, 1H, CCH_2), 5.35 (s, 1H, CCH_2), 5.21 (t, $J = 9.4$ Hz, 1H, H-3), 5.08 (t, $J = 9.8$ Hz, 1H, H-4), 5.01-4.96 (dd, $J = 8.0, 9.6$ Hz, 1H, H-2), 4.57 (d, $J = 7.9$ Hz, H-1), 4.27-4.23 (dd, $J = 4.8, 12.3$ Hz, 1H, H-6), 4.17-4.13 (dd, $J = 2.4, 12.3$ Hz, 1H, H-6'), 3.97-3.93 (m, 1H, $\text{OCH}_2\text{CH}_2\text{O}$), 3.73-3.40 (m, 8H, $\text{OCH}_2\text{CH}_2\text{O}$, H5, $\text{OCH}_2\text{CH}_2\text{N}_3$), 2.08, 2.03, 2.02, 2.00, 1.98 (s, 5x3H, 4x CH_3CO , CH_3); ^{13}C NMR (CDCl_3) δ 170.7, 170.3, 169.6, 169.5, 168.6, 140.2, 119.7, 101.0, 72.9, 72.1, 71.5, 70.1, 70.0, 69.1, 68.6, 62.1, 39.6, 20.9, 20.8, 20.7, 20.7, 18.8; ESI-MS: m/z calculated for $[\text{C}_{22}\text{H}_{33}\text{NO}_{12}\text{Na}]^+$, 526.1895, found 526.1888.

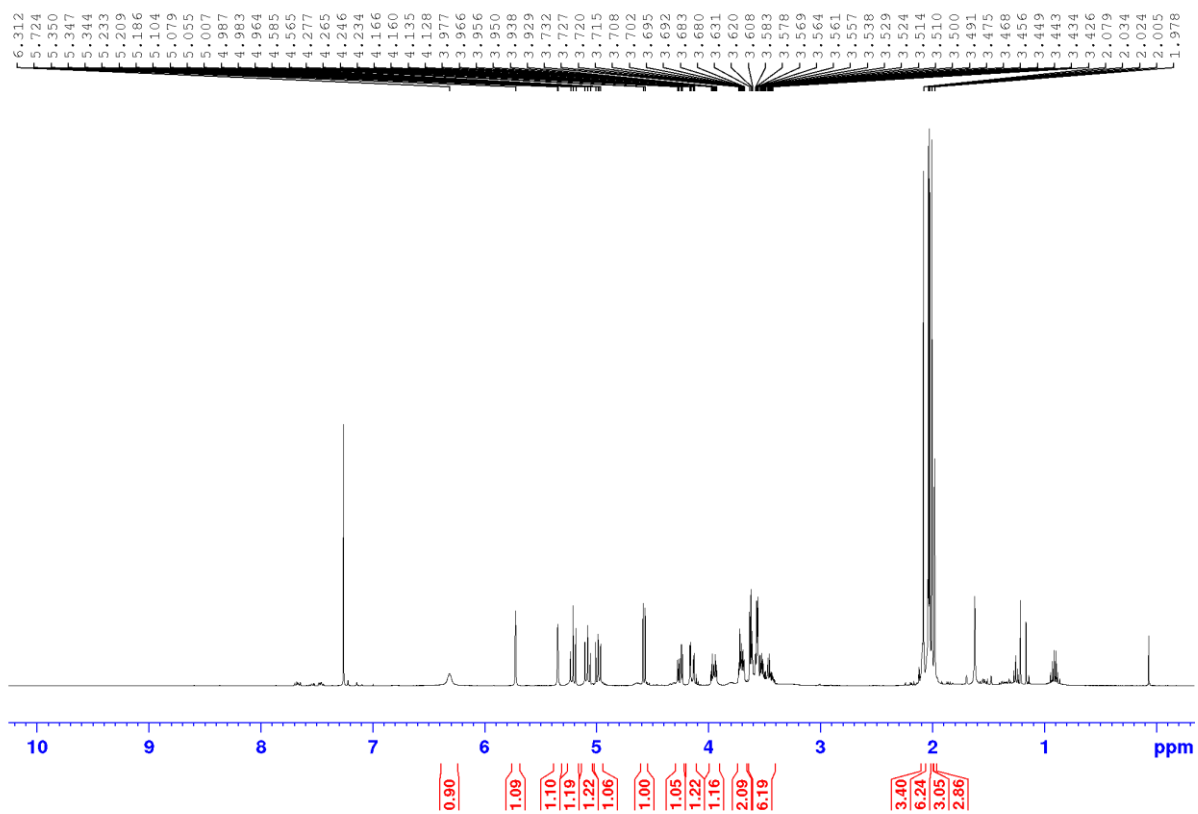


Figure S5: ^1H NMR of compound 3

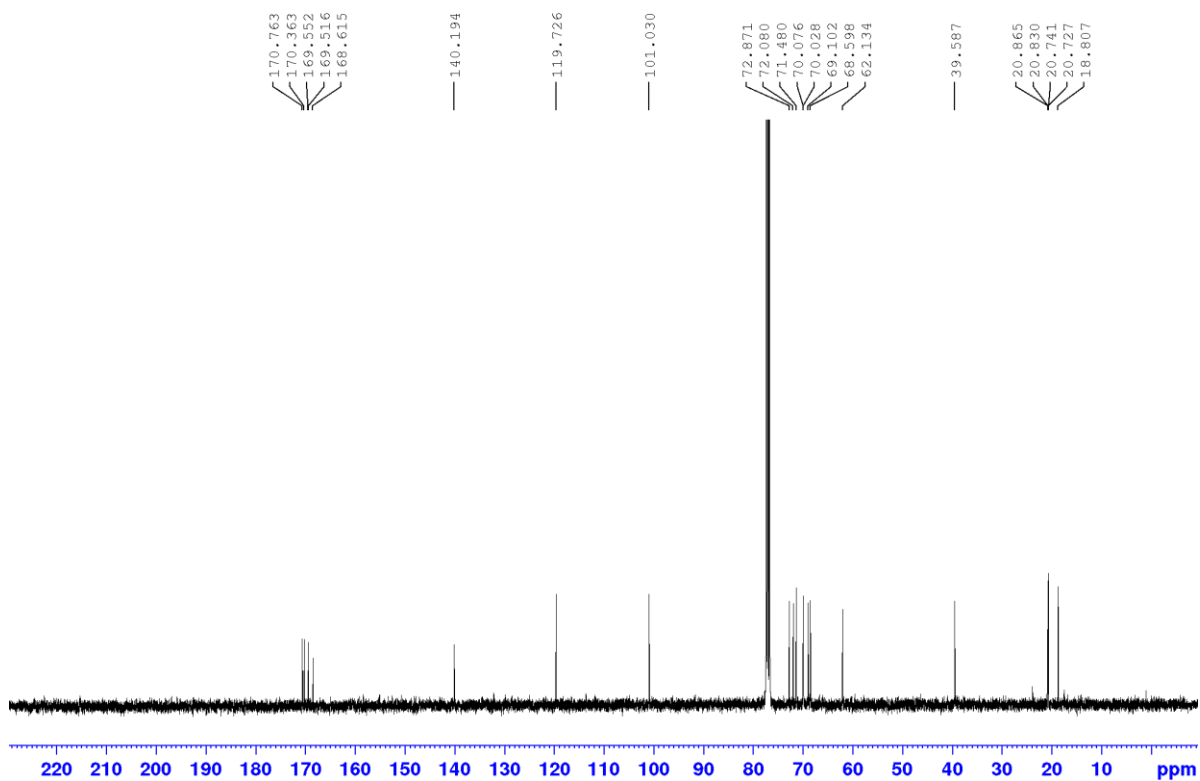


Figure S6: ^{13}C NMR of compound 3

The protected monomer (1.3 g, 2.6 mmol) was finally deacetylated in methanol (100 mL), using 1M NaOMe/MeOH solution (2 mL). The solution was stirred at room temperature for 3 h. The pH of the solution was adjusted to 5, the solution was then filtrated and the solvent was removed to obtain the pure monomer **4** as a colorless gum 0.8 g (98% yield).

^1H NMR (400 MHz, D_2O) δ 5.76 (s, 1H, CCH_2), 5.52 (s, 1H, CCH_2), 4.53 (d, $J = 8$ Hz, 1H, H-1), 4.13-3.32 (m, 14H, $\text{OCH}_2\text{CH}_2\text{O}$, H5, $\text{OCH}_2\text{CH}_2\text{N}_3$, H-2, -3, -4, -5, -6, -6'), 1.99 (s, 3H, CCH_3); ^{13}C NMR (D_2O) δ 173.2, 140.2, 122.1, 103.4, 77.0, 76.8, 74.2, 70.8, 70.6, 69.9, 69.8, 61.9, 40.2, 18.8; ESI-MS: m/z calculated for $[\text{C}_{14}\text{H}_{25}\text{NO}_8\text{Na}]^+$, 358.1472, found 358.1475.

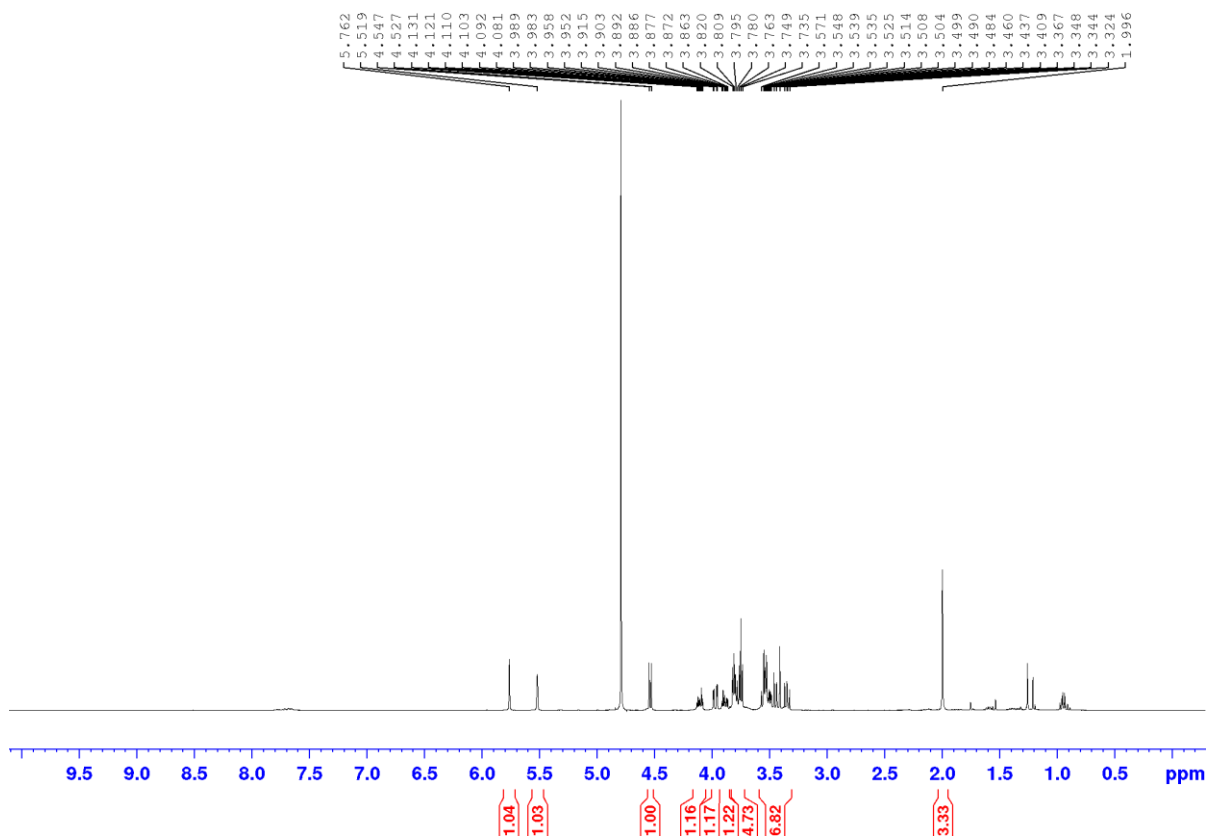


Figure S7: ^1H NMR of compound **4**

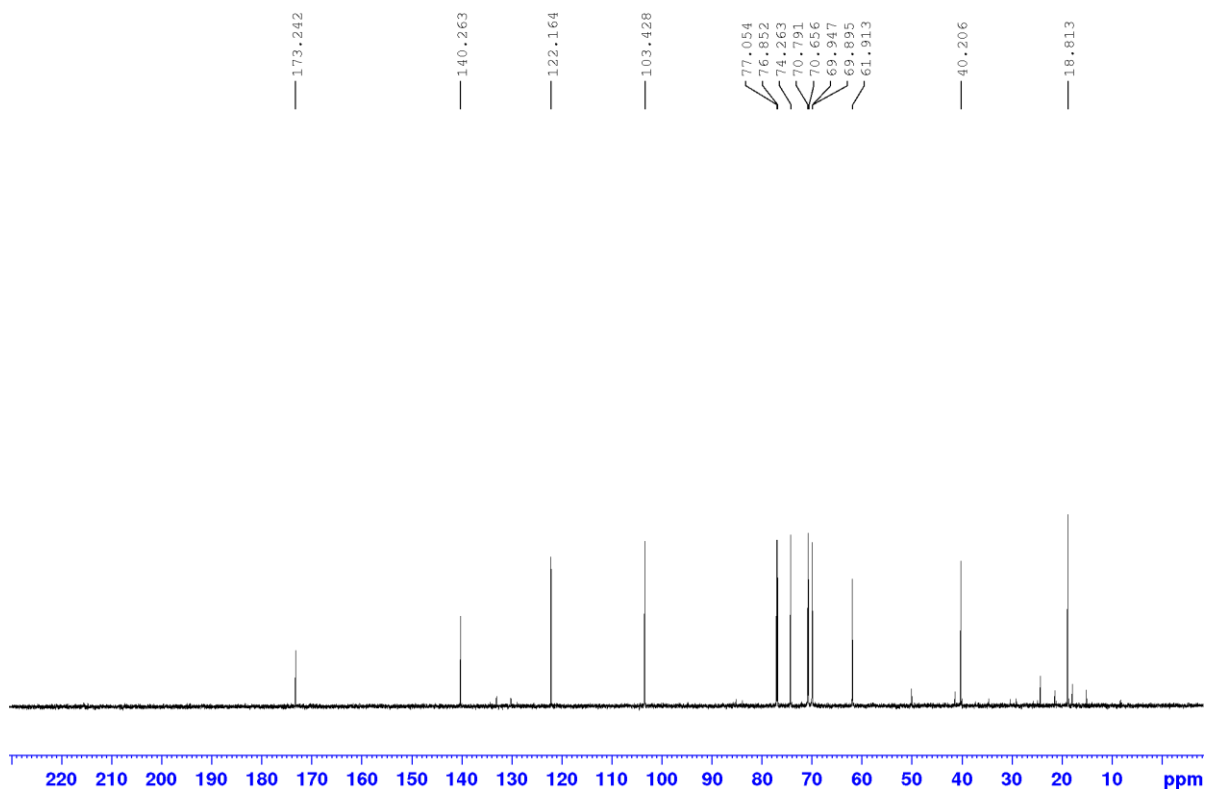


Figure S8: ^{13}C NMR of compound 4

Preparation of glyco-copolymers

Determination of Reactivity Ratios of HMM and GMA

Jaacks method was performed as described in literature². Feed ratio of co-monomers ($[\text{HMM}]_0/[\text{GMA}]_0$) are 34 and 0.028, respectively. The copolymerization was operated at 35 °C using CPADB as CTA and V70 as initiator ($[\text{HMM}+\text{GMA}]/[\text{CTA}]/[\text{Initiator}] = 50/1/0.2$). Kinetics studies of the polymerizations were systematically conducted and the conversions directly calculated by proton NMR spectra.

Kelen-Tüdös method was performed as described in literature³⁻⁴. The monomer feed ratio ($[\text{HMM}]_0/[\text{GMA}]_0$) was used at 0.25, 1 and 2. CPADB was selected as RAFT agent using V70 as initiator ($[\text{HMM}+\text{GMA}]/[\text{CTA}]/[\text{Initiator}] = 50/1/0.2$). The polymerizations were carried out at 35 °C. Again, kinetics studies of the polymerizations were systematically conducted and the conversions directly calculated by proton NMR spectra.

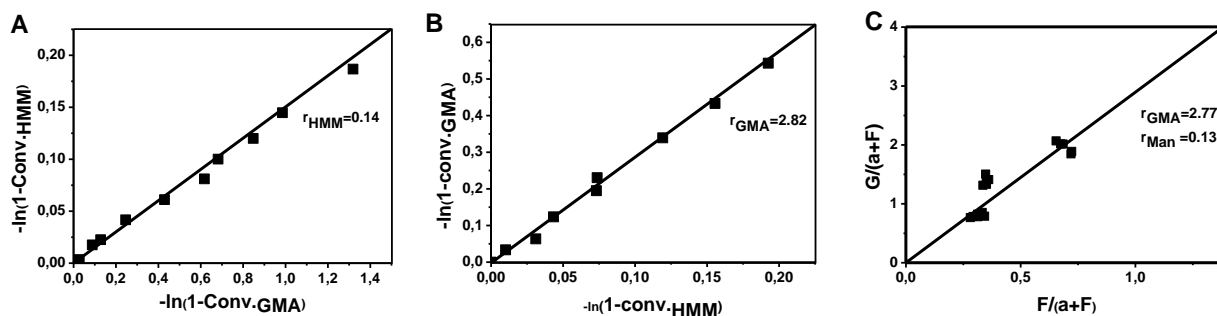


Fig S9. (A) Jaacks plots of the RAFT copolymerization at monomer ratio $[\text{HMM}]_0:[\text{GMA}]_0=34$; (B) Jaacks plots of the RAFT copolymerization at monomer ratio $[\text{HMM}]_0:[\text{GMA}]_0=0.028$; (C) Kelen-Tüdös plot for the RAFT copolymerization

of HMM and GMA in DMSO at 35 °C ($\alpha=0.57$).

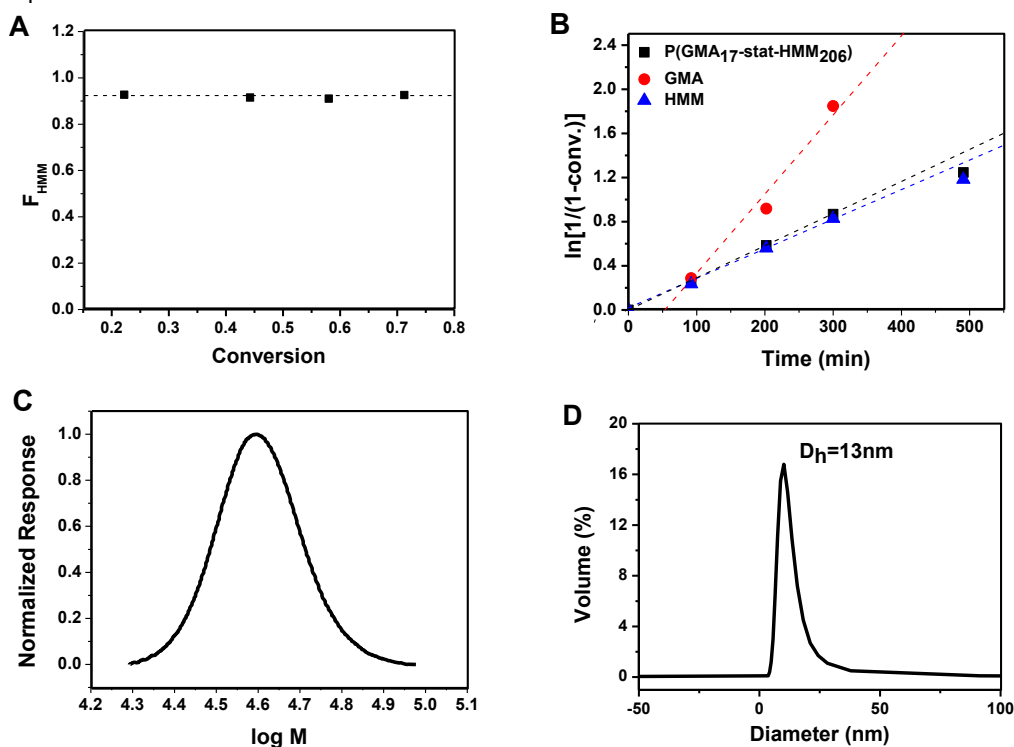
Preparation of Statistical Copolymer P (HMM-*stat*-GMA) via RAFT polymerization

In a typical experiment, a Schlenk flask (10 mL) was charged with HMM (120 mg, 0.33 mmol), GMA (1 mg, 0.007 mmol), 4,4'-azobis (4-cyanovaleric acid) (ACPA, 0.17 mg, 0.61×10^{-6} mol) and 4-cyano-4-(phenyl carbonothioylthio) pentanoic acid (0.33 mg, 1.18×10^{-6} mol) dissolved in 0.4 mL of anhydrous DMSO. After mixing, the pink solution was deoxygenated by three consecutive freeze-pump-thaw cycles. After the last cycle, the Schlenk flask was filled with argon, allowed to warm to room temperature and finally immersed in an oil bath at 70 °C. After 92 minutes, GMA (3 mg, 0.02 mmol) in DMSO solution (3 times freeze-pump-thaw cycles and protected by argon) was introduced into the flask by syringe pump ($v = 0.0378$ mL/h). After polymerization (conversion at 72%), the Schlenk flask was plunged into iced water and the solution was then freeze-dried overnight. The crude product was redissolved in a minimal quantity of methanol and precipitated in an acetone/petroleum ether mixture (volume ratio at 7/3) to remove unreacted monomer and initiator. The resulting pink powder was dried overnight under vacuum to give P(HMM-*stat*-GMA) as a pale pink solid. The different characteristics of the two polymers are summarized in **Table S1** and **Figure S10**.

Table S1: Glycopolymers obtained by RAFT polymerization

Polymer	[HMM+GMA]/[CTA]/[Initiator]	Conv (%)	$M_{n\ th}^a$ (kg.mol ⁻¹)	$M_{n\ NMR}^b$ (kg.mol ⁻¹)	M_n^c (kg.mol ⁻¹)	\mathcal{D}^d	D_h^e (nm)
P (HMM ₂₀₆ - <i>stat</i> -GMA ₁₇)	300/1/0.5	72	74.0	77.1	38.6	1.10	13

^a) calculated from monomer conversion; ^b) determined from relative integration of the aromatic chain end group and polymer backbone peaks; ^c) determined from SEC analysis in THF solution after acetylation of the glycopolymers (PS calibration); ^d) \mathcal{D} from SEC analysis in THF solution after acetylation of the glycopolymers; ^e) determined from DLS analysis in pure water.



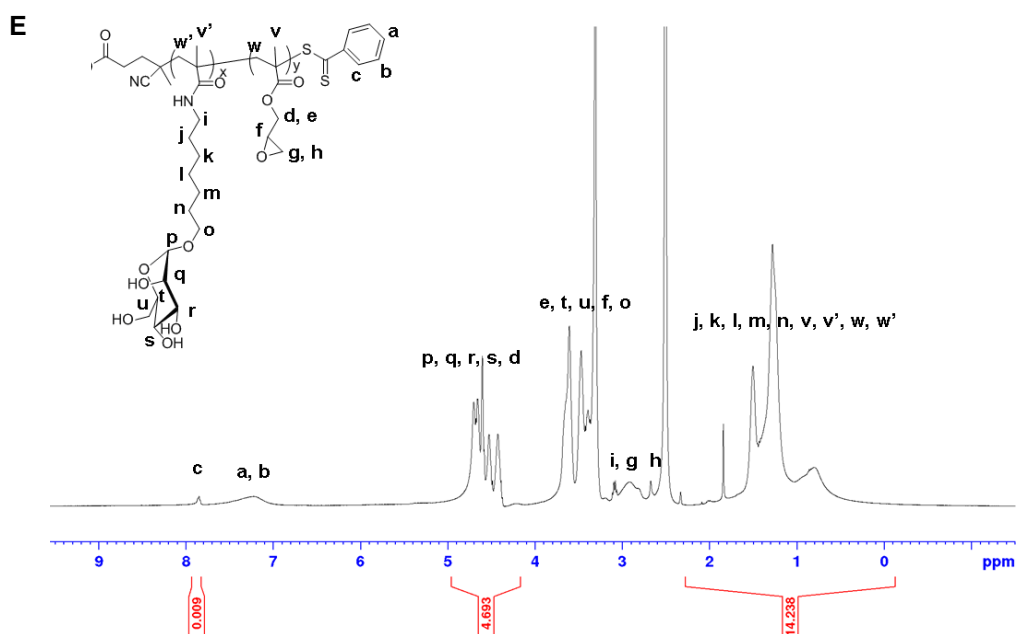


Fig S10. (A) Evolution of HMM mole fraction in the copolymer chain during the polymerization; (B) Pseudo first-order kinetic plots for GMA/HMM copolymerization (experimental details of GMA/HMM copolymerization given in page 3). (C) SEC traces of the glycopolymer after acetylation (THF, PS calibration); (D) Hydrodynamic diameters as measured by DLS in pure water (1 mg/mL); (E) ^1H NMR of glycopolymer in $\text{DMSO-}d_6$.

RAFT Polymerization of 4

Polymerization of **4** (60 mg) was performed in DMSO (0.5 mL) in the presence of 4-cyano-4-(phenylcarbonothioylthio) pentanoic acid as CTA (0.2 mg) and 4,4'-azobis (4-cyanovaleric acid) (0.06 mg) as initiator ($[\text{M}]_0/[\text{CTA}]/[\text{ACPA}]=250/1/0.3$). The solution was deoxygenated by three consecutive freeze-pump-thaw cycles and the Schlenk tube was finally filled with nitrogen, allowed to warm to room temperature and finally immersed in an oil bath at 70 °C. After polymerization (92% of conversion), the Schlenk tube was plunged into iced water and the solution was then freeze-dried overnight. The crude product was dissolved in a minimal quantity of DMSO and precipitated in an acetone/petroleum ether mixture (Volume ratio at 7/3) to remove unreacted monomer and initiator. The powder was dried overnight under vacuum to give 35 mg of polymer as a pale pink solid. ($DP_n = 242$, $M_{n, \text{NMR}} = 81.1 \text{ kg mol}^{-1}$, $\bar{D} = 1.30$), SEC analysis was performed in THF solution after acetylation of the glycopolymer (PS calibration).

Phase diagrams' determination

Glycopolymer/Water/Acetone system

Cloud point boundary. This equilibrium limit corresponds to the solubility limit of the polymer in acetone-water mixtures. The method consists in titrating aqueous solutions of glycopolymer with acetone until the mixtures turn milky (generation of swollen micelles). Compositions at the cloud point line are deduced from the mass of acetone added at the onset of turbidity and at a given glycopolymer initial concentration (see **Figure S11A**).

Miglyol/water/acetone system

Binodal curve. This equilibrium limit corresponds to acetone/water compositions for which miglyol 812 is not soluble anymore. The method consists in titrating acetic solutions of miglyol with water until the mixtures turn milky, or even phase separate, through the generation of droplets (see **Figure S11B**).

“Ouzo limit”. This boundary curve separates the Ouzo domain, where stable miglyol nanodroplets can be formed, from the high concentration region where miglyol phase-separates from the mixture. Special requirements are made here to ensure reproducible measurements of the Ouzo limit: i) a non-ionic surfactant (Brij56) is added in the organic phase to stabilize the miglyol droplets once formed; ii) just after adding the required content of water, an extra load of water is rapidly poured to dilute the samples and avoid Ostwald ripening. The Ouzo limit is determined by measuring the number of counts by DLS, before and after filtrating the mixture with 1,20 μm polyethersulfone filters. Identical numbers of counts before and after filtration correspond to homogeneous emulsions of miglyol droplets, whereas a decreasing number of counts indicates a loss of micro-scale miglyol droplets on the filter (**Figure S11B**).

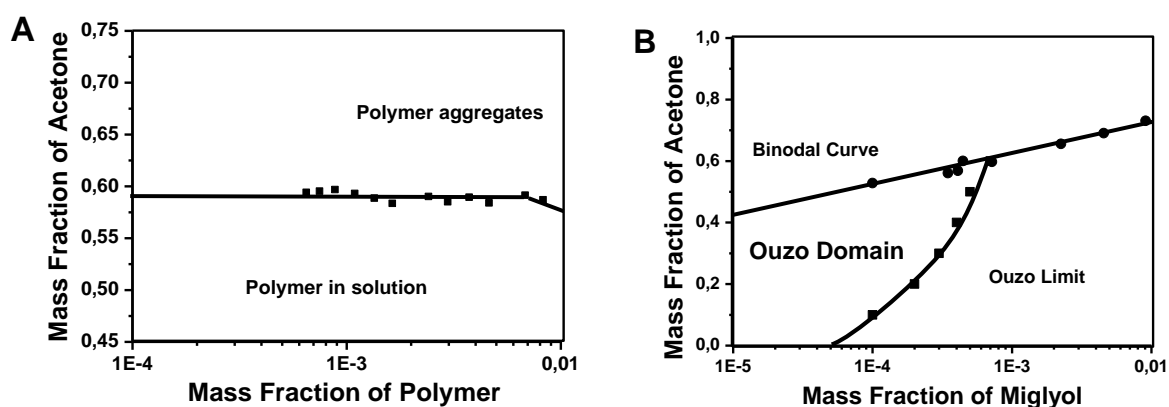


Fig S11: (A) Phase diagram of the copolymer in water/acetone mixtures. (B) Phase diagram of miglyol shifting in acetone/water mixture, showing the binary curve and the Ouzo limit. The content of water is deduced from the two other weight fractions.

Preparation of glyconanocapsules by co-nanoprecipitation/polymer crosslinking

Preparation of miglyol-filled nanocapsules (cystamine as cross-linker)

The glycopolymer (2.5 mg) was dissolved in 4.1 g of water, whereas 5 mg miglyol and 0.77 mg cystamine were poured in 5.9 g acetone separately. Polymer aqueous solution was then poured into the acetone solution all at once. The transparent solution turned to be milky immediately. The system was then put into an oil bath at 35°C for 1 day and characterized by TEM (**Figure S12**).

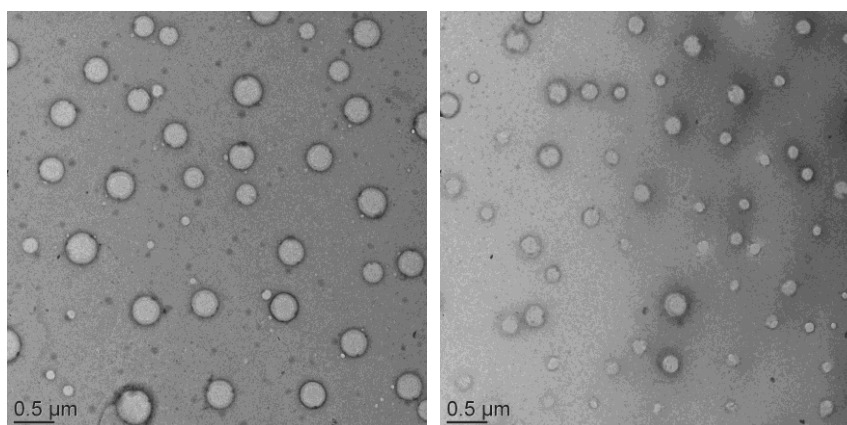


Fig S12. TEM pictures of two batches of glyconanocapsules cross-linked by cystamine, emphasizing the deficient reproducibility of the cross-linking reaction.

Preparation of miglyol-filled nanocapsules (IPDI as cross-linker)

Typically, the glycopolymer (2.5 mg) was dissolved in 4.1 g of water. In a second vial, 5 mg miglyol were added to 5.9 g acetone. Polymer aqueous solution was then poured into the acetone solution all at once, the transparent solution turned to be milky immediately. To prepare cross-linked nanocapsules, various contents of IPDI were added primarily in the acetone phase prior solvent shifting. The solutions were left overnight and further characterized by DLS and TEM (**Figure S13**).

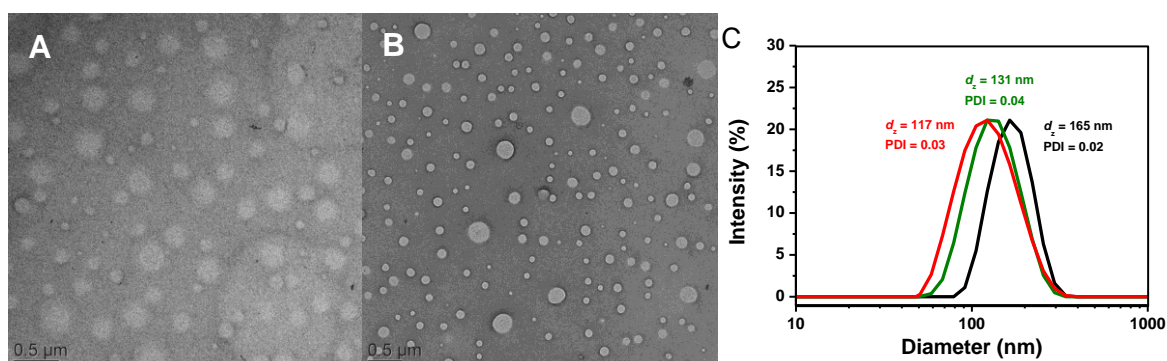


Fig S13: Selected TEM pictures of glyconanocapsules cross-linked with 8 and 24 equivalents (A and B, respectively) of IPDI per polymer chain. (C) DLS of glyconanocapsules cross-linked with 8 (black), 24 (green) and 48 (red) equivalents of IPDI (per polymer chain).

Hexadecane-filled Nanocapsules (IPDI as cross-linker)

The domain for capsules preparation was obtained by overlapping hexadecane (HD)/acetone/water and polymer/acetone/water phase diagrams (**Figure S14**). HD-filled nanocapsules were reproducibly generated in the green region of the figure. In a typical experiment, the glycopolymer (2.5 mg) was dissolved in 4.1 g of water whereas 5 mg of HD and IPDI (48 eq. per chain, 0.36 mg) were dissolved in 5.9 g of acetone separately. Polymer aqueous solution was then poured into the acetone solution all at once. The solution was left overnight and then characterized by DLS and TEM (**Figure S15**).

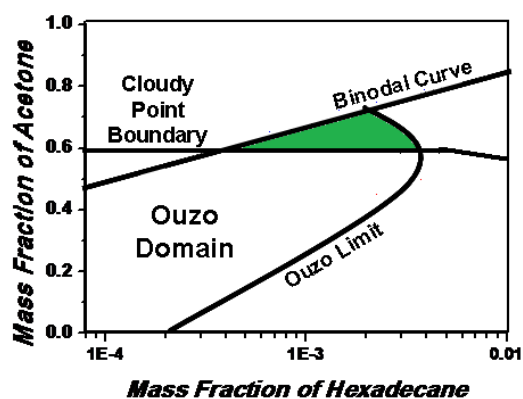


Fig S14. Overlapped phase diagram of copolymer and HD in acetone/water mixtures. The green domain corresponds to the range of compositions where well-defined nanocapsules are generated.

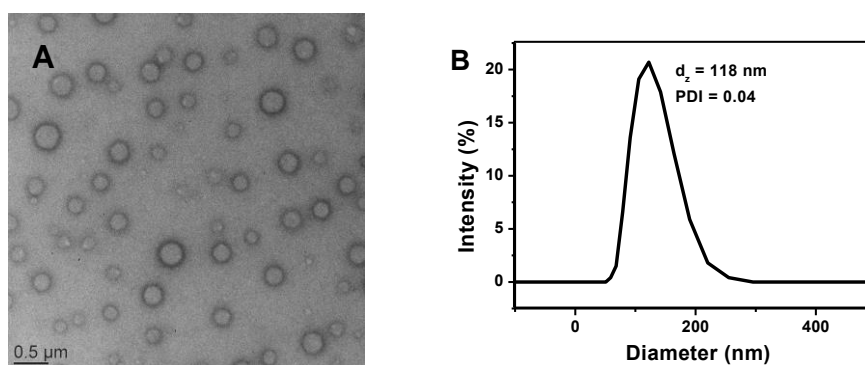


Fig S15. (A) TEM image of HD-filled nanocapsules; (B) DLS measurement of HD-filled nanocapsules in conditions of nanoprecipitation (water/acetone mixture).

Encapsulation of hydrophobic active components

Pyrene-Loading experiment. The glycopolymer (2.5 mg) was dissolved in 4.1 g of water. 5 mg of miglyol containing 2.5% wt pyrene and 0.36 mg of IPDI (48 eq per polymer chain) were dissolved in 5.9 g of acetone. The polymer aqueous solution was then poured into the acetone solution and the solution was left overnight. After dialysis against water for 3 days, the solution was analyzed by fluorescence spectroscopy and DLS (**Figure S16**).

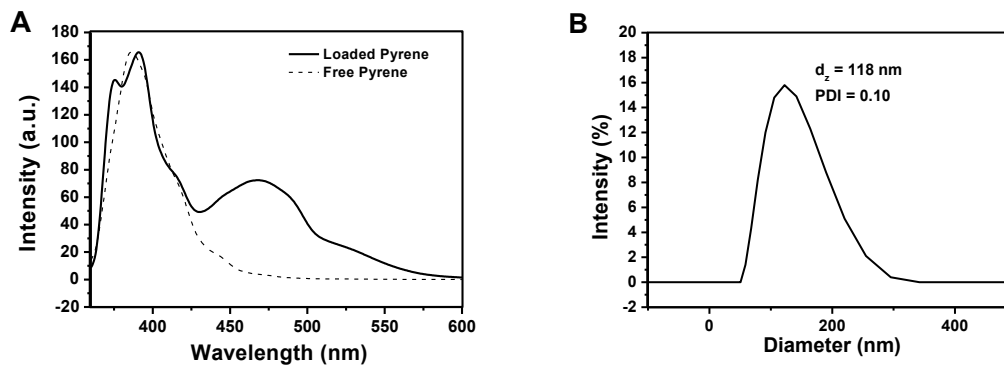


Fig. S16. (A) Fluorescence emission spectra of Pyrene-loading glyconanocapsules. The straight line shows the loaded pyrene glyconanocapsules, the dash line corresponds to the reference (free pyrene at same concentration in miglyol). The presence of a clear excimer peak (from 460 nm to 550 nm) for the pyrene-loaded sample confirms the hydrophobic environment of pyrene molecules embedded in miglyol oil. (B) DLS measurement of pyrene-loaded

nanocapsules.

Flumequine-Loading experiment. The glycopolymer (2.5 mg) was dissolved in 4.1 g of water. 5 mg of Miglyol containing 0.03% wt of Flumequine and 0.36 mg of IPDI (48 eq per polymer chain) were dissolved in 5.9 g of acetone. The polymer aqueous solution was then poured into the acetone solution and the solution was left for overnight. After dialysis for 3 days, the glyconanocapsule solution was analyzed by Fluorescence spectroscopy (**Figure S17**).

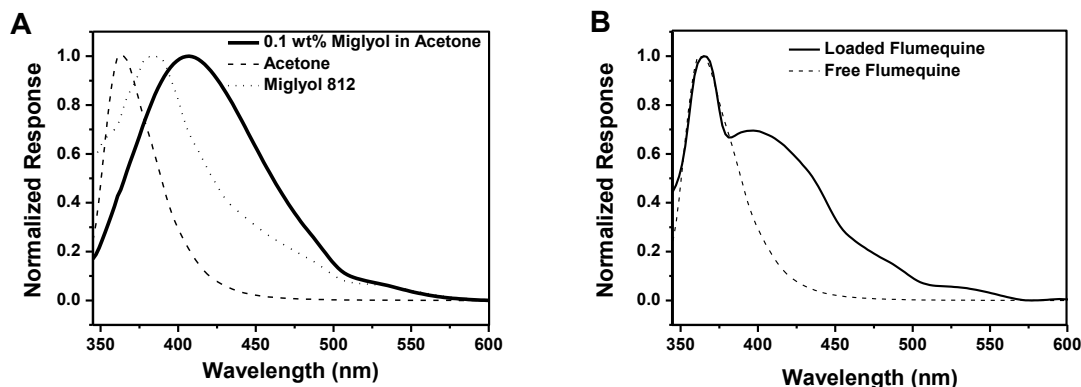


Fig. S17. (A) Fluorescence emission spectra of Flumequine in different solvents ($\lambda_{exc} = 325$ nm). (B) Fluorescence emission spectra of Flumequine-loading glyconanocapsules. The straight line shows the spectrum of a dispersion of Flumequine-loaded glyconanocapsules and the dash line corresponds to a solution of free Flumequine.

Post-nanoprecipitation modification

Functionalization of glyconanocapsules using amino-functionalized biotin. The glycopolymer (2.5 mg) was dissolved in 4.1 g of water. 5 mg of miglyol and 0.36 mg IPDI (48 eq per polymer chain) were dissolved in 5.9 g of acetone. The polymer aqueous solution was then poured at once into the acetone solution to generate glyconanocapsules. After one night, 0.01 mg of amino-functionalized biotin (1 eq per chain) was added into solution and reacted at 40 °C overnight. After dialysis for 3 days, 0.125 eq. avidin in 0.5 mL water was added into the glyconanocapsule solution and the evolution of the aggregated complex was analyzed by DLS. In the meantime, the dialyzed sample was measured by UV-Vis after introducing HAVA/Avidin reagent for determining the efficiency of biotin grafting reaction (**Figure S18**).

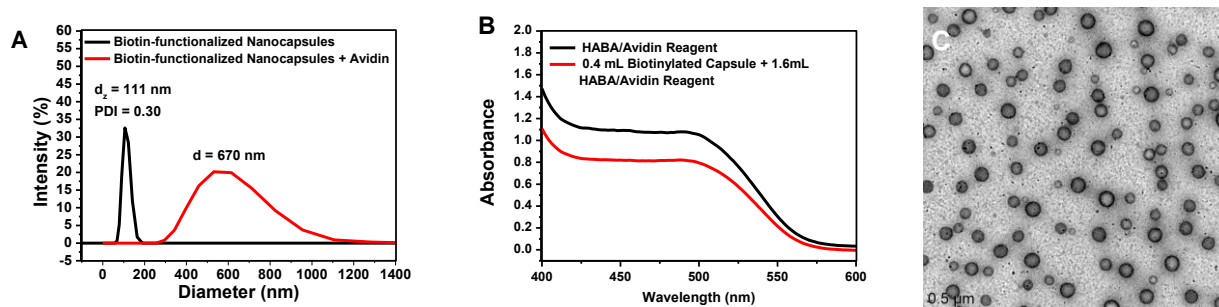


Fig S18. (A) Size distribution of biotinylated nanocapsules in water before and after conjugation to avidin. (B) UV-absorption spectra of biotinylated and non-biotinylated nanocapsules. HABA test results were calculated using absorbances measured at 500nm. (C) TEM picture of the biotin-functionalized glyconanocapsules.

Functionalization of glyconanocapsules using Alexa Fluor® 555 Cadaverine. The glycopolymer (2.5 mg) was dissolved in 4.1 g of water. 5 mg of miglyol and 0.36 mg of IPDI (48 eq per polymer chain)

were dissolved in 5.9 g of acetone. The polymer aqueous solution was then poured into the acetone solution to generate glyconanocapsules. After one night, 0.003 mg of Alexa Fluor 555 Cadaverine (0.1 eq per chain) was added into solution and reacted overnight at 40 °C. The glycocapsules were characterized by DLS and TEM (**Figure S19**). The glycocapsules were purified by dialysis against water and subsequently characterized by fluorescence spectroscopy.

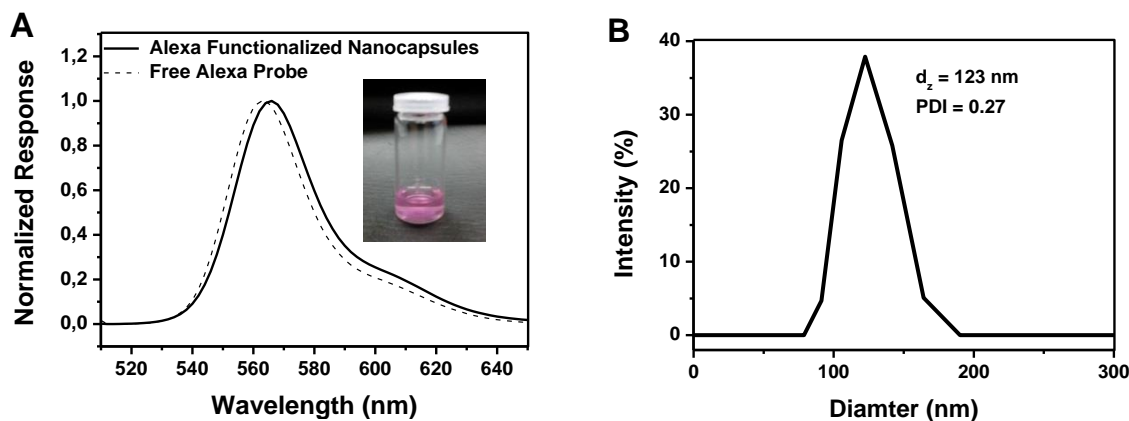


Fig S19. (A) Fluorescence emission spectra of Alexa-functionalized glyconanocapsules. (B) Size distribution of Alexa-functionalized nanocapsules.

Functionalization of glyconanocapsule using amino-functionalized magnetic particles. The glycopolymer (2.5 mg) was dissolved in 4.1 g of water. 5 mg of miglyol and 0.36 mg IPDI (48 eq per polymer chain) were dissolved in 5.9 g of acetone. The polymer aqueous solution was then poured into the acetone solution to generate glyconanocapsules. After one night, 0.02 mL of amino-turbobead (30 mg/mL) was added into the solution and reacted overnight at 40 °C. The magnetic NP-grafted nanocapsules were characterized by DLS and TEM (**Figure S20**). Purification of the nanocapsules was performed through magnetic separation (x 3 aqueous solution).

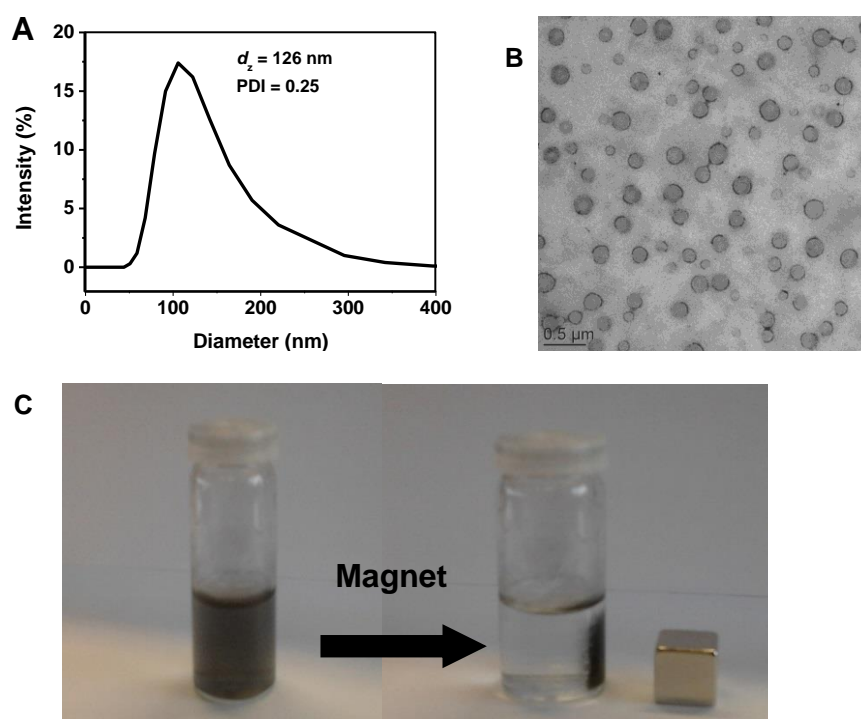


Fig S20. (A) Size distribution of magnetic NP-grafted glyconanocapsules. (B) TEM picture of the magnetic NP-grafted glyconanocapsules. (C) Behavior of magnetic NP-grafted glyconanocapsules in the presence of a magnet

Cytotoxicity tests

Cell culture was performed at 37°C and 5.0% CO₂ in RPMI 1640 medium supplemented with 10% FCS, 1% glutamine, 1% penicillin-streptomycin (all from Invitrogen Life Technologies, Karlsruhe, Germany). Cell death was induced in Jurkat and HeLa cells by UV-B irradiation, 180 mJ/cm² followed by 24h incubation period. Glyconanocapsules were added to cell culture at the concentration up to 10 µg/mL and were co-incubated for 24h.

Cells' death changes their morphology. Cell apoptosis provokes cellular shrinkage and an increased cytoplasmic granularity and vacuolization, which are reflected by a decrease in forward scatter (FSC) and an increase of side scatter (SSC) of a cell population. In addition the following parameters were encountered: surface exposure of phosphatidyl serine (detected by annexinV-FITC binding), membrane integrity (detected by propidium iodine staining), DNA content (detected by Hoechst 33342 staining) and mitochondrial membrane potential (detected by DiIC1(5) staining). Combination of named six parameters allows discrimination of viable, stressed, early apoptotic, apoptotic, late apoptotic, primary necrotic, secondary necrotic and late secondary necrotic cells as described in details in the literature⁵⁻⁶.

100 µl of cell suspension containing 10⁵ cells were incubated with 400 µl of freshly prepared 4-colour staining solution (1µg/ml AxV5-FITC, 20µg/ml PI, 10nM DiIC1(5), 1µg/ml Hoechst 33342 in Ringer's solution) and subsequently analyzed by flow cytometry. Flow cytometry was performed with a Gallios cytofluorometer (Beckman Coulter, Fullerton, CA, USA). Excitation for FITC and PI was at 488 nm, the FITC fluorescence was recorded on FL1 sensor (525/38 nm BP), the PI fluorescence on FL3 sensor (620/30 nm BP), the DiIC1(5) fluorescence was excited at 638nm and recorded on FL6 sensor (675/20 nm BP), and the Hoechst 33342 fluorescence was excited at 405 nm and recorded on FL9 sensor (430/40 nm BP). Data analysis was performed with Kaluza software version 1.3 (Beckman Coulter, Fullerton, CA, USA).

Results obtained by flow cytometry indicated that cell death rate after treatment with nanocapsules was not different from those in the population of untreated cells, while irradiation with UV-B served as positive control of cell death and resulted in accumulation of different forms of dying cells as can be seen from **Figure S21**.

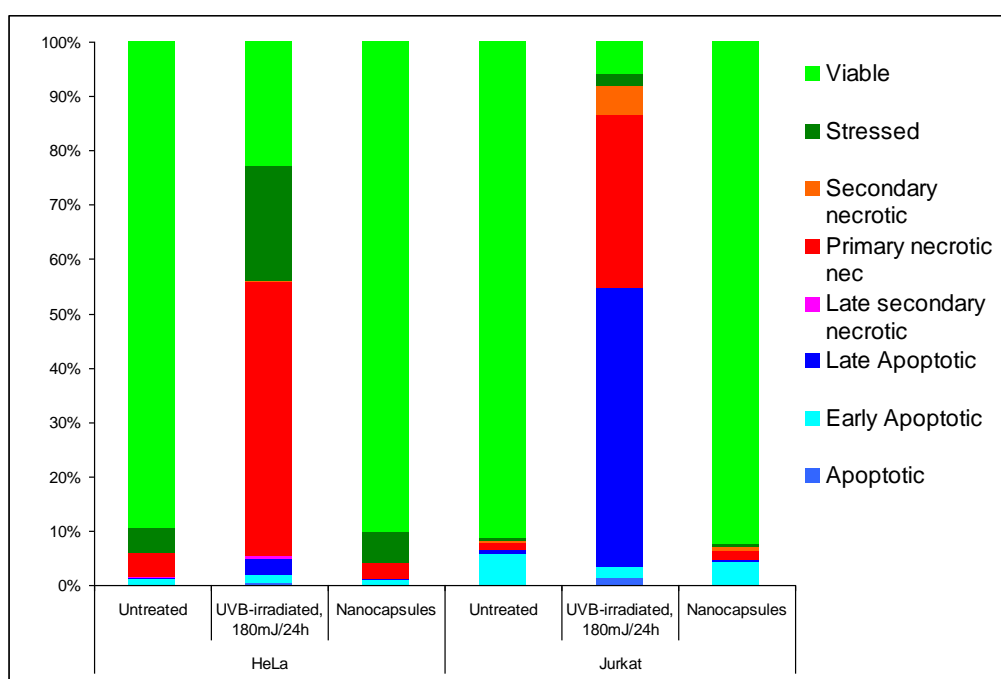


Fig S21. Cytotoxicity tests on nanocapsules, incubated with human HeLa and Jurkat cells for 24h at 10µg/ml of culture medium. Untreated cells served as negative control, while UV-B irradiated cells served as positive control for cells death. Cells were evaluated for cell shape changes (FSc/SSc) as well as AnnexinV/PI/Hoechs33332/DIIC5 6-parameter flow cytometry to discriminate different stages of cells death. Each graph is a mean of 3 independent experiments, each including at least 10 000 analyzed cells.

Mannosylated Glyconanocapsules induced Bacteria Aggregation

E. Coli AIEC LF82 marked with GFP was incubated in the medium to produce a batch of bacteria solution ($OD_{620nm} = 0.6$). After evaporation of acetone, the aqueous solution of mannosylated glyconanocapsules was concentrated to 33 and 66 µM. 10 µL of capsules solution was then added into 10 µL bacteria solution and the solution was placed on a stirring table. After 3h of incubation, the bacteria were observed by confocal fluorescence microscopy.

Kinetic study on capsules/bacteria aggregation was also performed in a similar process as above. 10 µL of 66 µM capsules solution was added into 10 µL bacteria solution and the solution was stirred gently. The observation of aggregates by confocal microscopy was performed after 30 min, 1 h, 2 h and 3 h of incubation.

The same procedure was operated for co-incubation of GFP-marked AIEC LF82 and AFC-functionalized glyconanocapsules (Figure 3 in the main text and **Figure S22**).

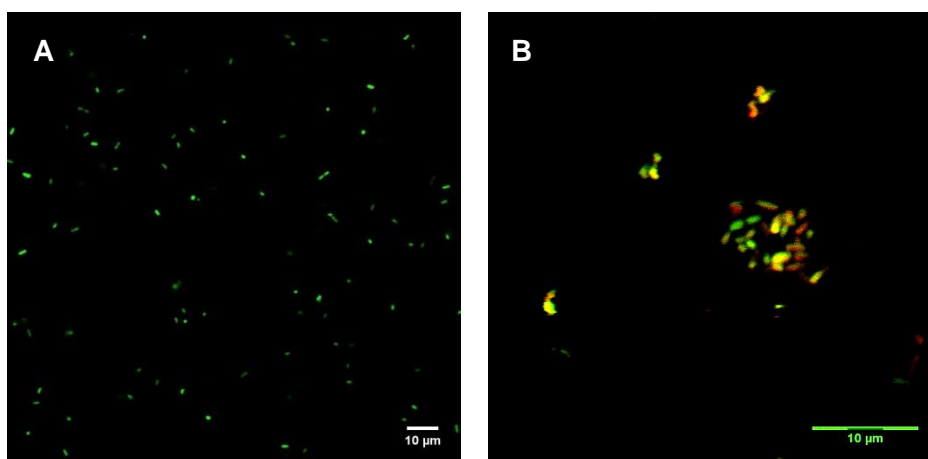


Fig. S22. Confocal fluorescence microscopy (CFM) picture of (A) GFP-marked AIEC LF82 standing for 3h as a control test and (B) GFP-marked AIEC LF82 incubated with AFC-functionalized mannosylated glyconanocapsules for 2h (the photo shows overlapped fluorescence) (GFP: green fluorescence, AFC:red fluorescence).

Removal of bacteria

E. coli AIEC LF82 marked with GFP was incubated in the medium to produce a batch of bacteria solution ($OD_{620nm} = 0.6$). After transferring 100µL of bacteria into a vial, 100 µL of magnetic glyconanocapsules aqueous solution (5mg of polymer/mL) were then added into bacteria solution and incubated for 3 h on a stirring table. Then, a magnet was set at the bottom of the vial for 1 min to induce a magnetic-driven precipitation. Keeping the presence of magnet at the bottom of the vial, we removed the upper part of the solution (S1) and washed the precipitates with water for 3 times. Afterwards, the magnet was removed and the precipitate was redispersed with 100 µL of water for confocal fluorescence microscopy analysis (Fig. 3, main text). The upper part of solution (S1, magnetic nanocapsules-free solution) was diluted and plated

onto LB agar plates to determine the number of colony-forming units (CFU), the initial bacteria solution (standing for 3h, S0) was used as reference. The removal efficiency (83%) was calculated from comparison of CFU population between in S1 and reference bacteria solution (S0).

Residual adhesion

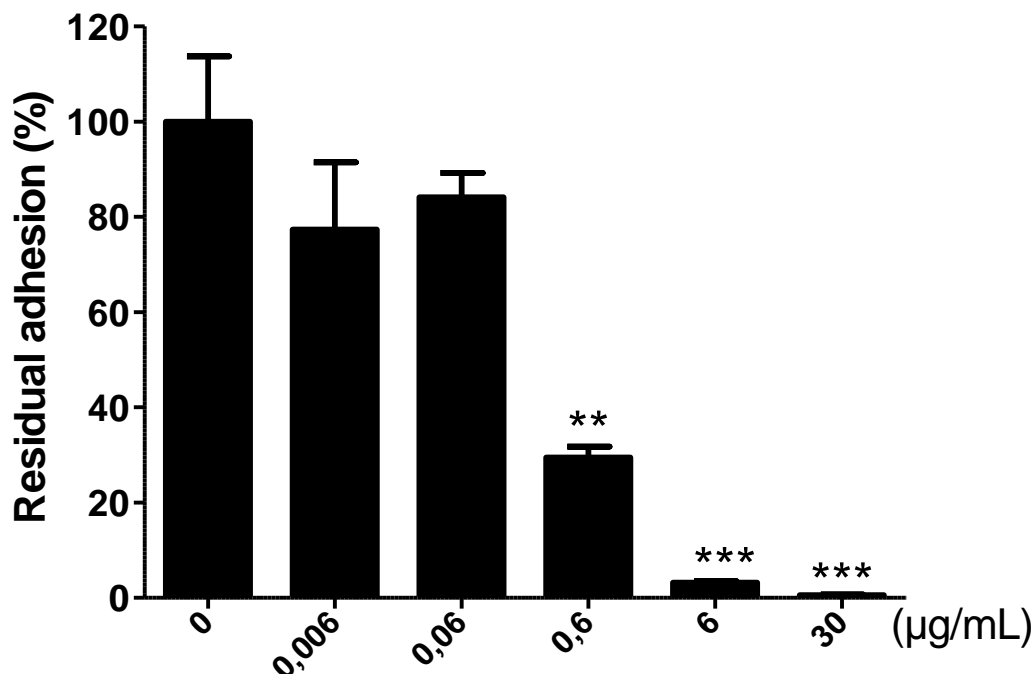


Fig S23. Inhibitory effects of HM-GC on AIEC LF82 adhesion levels to T84 cells in preincubation experiments

Control experiment

Preparation of Glucose-based nanocapsules

The glucose-functionalized glycopolymer (0.5 mg) was dissolved in 500 mg of water, whereas 0.3 mg miglyol 812 and 24 eq. IPDI were poured in 500 mg acetone. Polymer aqueous solution was then incorporated into the acetone solution all at once. The transparent solution turned to be milky immediately (Figure S24).

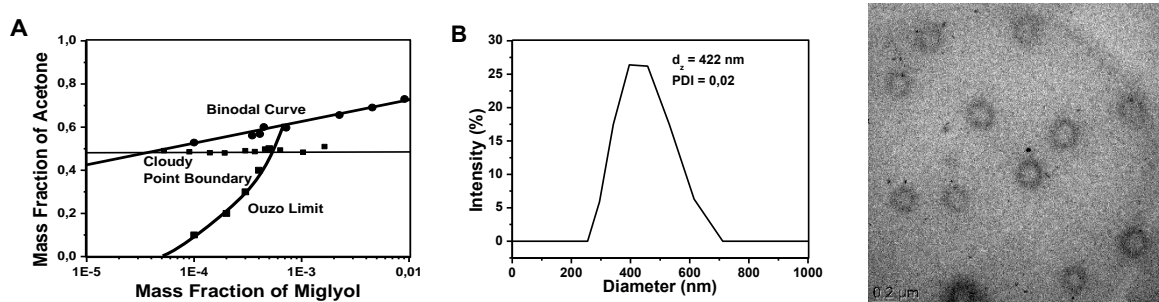


Fig S24. (A) Overlapped phase diagram of glucose-functionalized glycopolymer and miglyol in acetone/water mixtures; DLS (B) and TEM picture (C) of IPDI-cross-linked glucose based nanocapsules.

Incubation of AIEC LF 82 with Glucose based Glyconanocapsules

An aqueous solution of glucose-based nanocapsules (10 μ L at 66 μ M) was added to 10 μ L of GFP marked *E. coli* AIEC LF82 solution ($OD_{620nm} = 0.6$) and the solution was placed on a stirring table. After 3h of incubation, the bacteria were observed by confocal fluorescence microscopy (**Figure S25**). No cluster was observed.

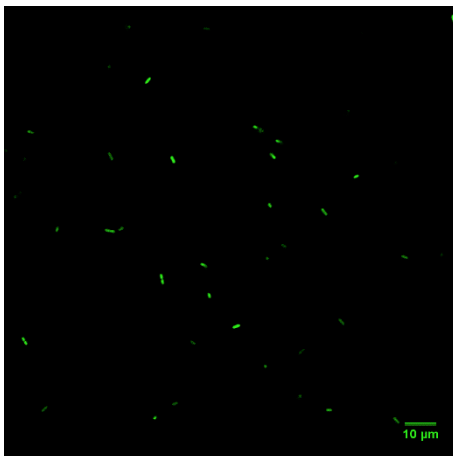


Figure S25. Confocal fluorescence microscopy (CFM) picture of GFP-marked AIEC LF82 after 3h of incubation with glucose-based capsules (66 μ M).

References

1. X. Yan, M. Delgado, A. Fu, P. Alcouffe, S. G. Gouin, E. Fleury, J. L. Katz, F. Ganachaud and J. Bernard, *Angew. Chem. Int. Ed.*, 2014, **53**, 6910.
2. V. Jaacks, *Die Makromolekulare Chemie*, 1972, **161**, 161.
3. T. Kelen, F. Tüdös and B. Turcsanyi, *Polymer Bulletin*, 1980, **2**, 71
4. T. Kelen, F. Tüdös and B. Turcsanyi, *Journal of Polymer Science: Polymer Chemistry Edition*, 1977, **15**, 3047.
5. L. E. Munoz, C. Maueroeder, R. Chaurio, C. Berens, M. Herrmann and C. Janko, *Autoimmunity*, 2013, **46**, 336.
6. C. Janko, L. Munoz, R. Chaurio, C. Maueroeder, C. Berens, K. Lauber and M. Herrmann, *Methods in Molecular Biology*, 2013, **1004**, 3.